Eur. Phys. J. A **18**, 697–709 (2003)
DOI 10.1140/epja/i2003-10060-0

THE EUROPEAN PHYSICAL JOURNAL A

Scalar-meson production in nucleon-nucleon collisions near threshold

M.P. Rekalo[1,a] and E. Tomasi-Gustafsson[2,b]

[1] Middle East Technical University, Physics Department, Ankara 06531, Turkey
[2] DAPNIA/SPhN, CEA/Saclay, 91191 Gif-sur-Yvette Cedex, France

Received: 1 April 2003 /
Published online: 11 November 2003 –
Communicated by V.V. Anisovich

Abstract. We establish the model-independent spin structure of the matrix elements for the near-threshold scalar-meson production in pp and np collisions, when the final particles are emitted in S-state. Polarization phenomena are derived in a general form. The properties of the t-channel dynamics, which is based on different meson exchanges, are studied in terms of the s-channel parametrization of the matrix element. The predictions of a model, based on $\pi + \sigma$ exchanges are also presented.

PACS. 13.75.Cs Nucleon-nucleon interactions (including antinucleons, deuterons, etc.) – 21.10.Hw Spin, parity, and isobaric spin – 13.88.+e Polarization in interactions and scattering

1 Introduction

The strong and electromagnetic decays of the scalar mesons S ($S = \sigma$, f_0, and a_0) have been recently the object of great theoretical and experimental interest. The structure of these mesons is not yet fully understood and the coupling constants of their decays are not determined (see [1–8] and references therein). As an example, the electromagnetic constants $g_{\rho\sigma\gamma}$ and $g_{\omega\sigma\gamma}$ are very important for the solution of different problems in hadron electrodynamics. The constant $g_{\rho\sigma\gamma}$ drives the σ contribution to the differential cross-section of the process $\gamma + p \to p + \rho^0$ [9–11] in the near-threshold region. The coupling constant $g_{\omega\sigma\gamma}$ is important for the estimation of the effects of the meson exchange currents for the deuteron electromagnetic form factors [12–14], particularly in the region of large momentum transfer. Both these constants play a major role in the interpretation [15] of the HERMES effect [16], concerning the anomalous behavior of the electroproduction cross-section on nuclei at low Q^2, where the cross-section is enhanced for longitudinally polarized virtual photons and depleted for transversally polarized photons. Moreover, the constants $g_{\rho\sigma\gamma}$ and $g_{\omega\sigma\gamma}$ enter in the interpretation of different radiative decays of vector mesons, like $\rho^0(\omega) \to \pi^0\pi^0\gamma$ and $\rho^0(\omega) \to \pi^+\pi^-\gamma$ [17].

Two-photon decays of scalar mesons, $S \to 2\gamma$, which are important for the estimation of the corresponding t-channel contributions to the amplitudes of real and virtual Compton scattering on nucleons [18–21], can be estimated on the basis of the $g_{V\sigma\gamma}$ coupling constants, in the VDM approach.

In the framework of the effective Lagrangian approach, the calculation of the cross-section for scalar-meson photo- and electroproduction on nucleons requires the knowledge of the $g_{V\sigma\gamma}$ and g_{NNS}-coupling constants. The strong coupling constants g_{NNS} [22,23] enter in various calculations in hadron dynamics, not only with respect to the NN potential, but also for different observables for processes like $\pi + N \to S + N$ [24,25], $N + N \to S + d$ [25–28], and $N + N \to S + N + N$ [24].

The feasibility of the experimental study of scalar-meson production depends essentially on the nature and on the rate of the decay. If, for example, the decay $f_0 \to K\overline{K}$ or $a_0 \to K\overline{K}$ dominates, these mesons could be observed in the $K\overline{K}$ effective-mass distribution, close to the kaon mass, as a resonant contribution. Such effects have been observed in πN collisions [4,29–34]. The interpretation of the data needs an adequate theoretical approach for the process $\pi + N \to N + S^0$. It was shown that for $p + p \to p + p + K^+K^-$, in the kinematical conditions of the DISTO experiment [35] or at COSY the presence of the f_0 signal is hindered by a large background. Therefore, in principle, the process $n + p \to n + p + K^+K^-$ could be more favorable, because the cross-section is one order higher, whereas the background is comparable with respect to pp collisions.

Note that the experimental study of K^+K^- production in the process $p + p \to p + p + K^+ + K^-$, at an

[a] *Permanent address*: NSC-Kharkov Institute of Physics and Technology, 310108 Kharkov, Ukraine.
[b] e-mail: etomasi@cea.fr

energy excess $Q = 17$ MeV over threshold [36], gives the following value: $\sigma(pp \to ppf_0) = \left(1.84 \pm 0.29^{+0.25}_{-0.35}\right)$ nb, including the statistical and systematic errors. The extension of this study is foreseen [37–39].

In this paper we derive the most general and model-independent properties for the processes of scalar-meson production in NN collisions, in the threshold region, where the theoretical analysis is essentially simplified. The spin structure of the corresponding matrix elements contains a set of sixteen independent amplitudes in the general case, eight amplitudes for coplanar kinematics and only three independent amplitudes at threshold.

This paper is organized as follows. In sect. 2, using the selection rules with respect to the Pauli principle, P-parity and total angular momentum, we establish the spin structure of the matrix elements for the processes $p+p \to p+p+S^0$ and $n+p \to n+p+S^0$ and analyze the polarization phenomena for these processes in a model-independent way. In sect. 3 we convert the different t-channel contributions (described by a definite set of Feynman diagrams) into the universal s-channel parametrization. This gives the expression for the corresponding partial threshold amplitudes. In sect. 4 we discuss the predictions of a model based on $\sigma + \pi$ exchanges. The threshold amplitudes for the different subprocesses, $M^* + B \to N + S^0$ (where M^* is the virtual π-, f_0-, and V-meson) have been calculated in sect. 5, in the framework of the effective Lagrangian approach. Summing all possible t-channel contributions, we predict the threshold behavior of the total cross-section for the f_0- and a_0-meson production in pp collisions (sect. 6). A short discussion of final-state interactions (FSI) is done in sect. 7. The results are summarized in the conclusions.

2 Spin structure of the threshold matrix element and polarization observables

The spin structure of the matrix elements for scalar-meson production in NN collisions, $N + N \to N + N + S^0$, in the threshold region is determined by the selection rules with respect to P-parity, total angular momentum and by the Pauli principle. The threshold region, where all final particles in $N+N \to N+N+S^0$ are produced in relative S-state, can be rigorously described by a formalism based on the two-component nucleon spinor parametrization of the corresponding matrix element. This formalism can be built in a model-independent way [40], and has been previously successfully applied to vector [41], pseudoscalar [42], strange [43], J/ψ [44], and charm [45] particle production in nucleon-nucleon collisions.

Let us explicitly derive the matrix element for the processes $p + p \to p + p + S^0$, where S^0 denotes a neutral scalar meson, $S^0 = \sigma$, f_0 or a_0^0. Due to the Pauli principle, at the reaction threshold, only the quantum number $j^P = 0^+$ is allowed, where j is the total angular momentum and P is the P-parity of the colliding protons. One partial transition can take place, corresponding to

$$S_\mathrm{i} = 0,\ \ell = 0 \ \to\ j^P = 0^+ \ \to S_\mathrm{f} = 0, \qquad (1)$$

where S_i (S_f) is the total spin of the initial (final) protons and ℓ is the angular orbital momentum of the colliding protons.

The spin structure of the threshold matrix element for the transition (1), in the CMS of the considered reaction, can be parametrized in the following general form:

$$\mathcal{M}_{pp} = g(\chi_4^\dagger \sigma_y \tilde{\chi}_3^\dagger)(\tilde{\chi}_2 \sigma_y \chi_1), \qquad (2)$$

where χ_1 and χ_2 (χ_3 and χ_4) are the two-component spinors of the initial (final) protons; g is the threshold partial amplitude, describing the singlet-singlet transition in the pp-system (with scalar-meson production in the S-state), which is generally a complex function of three independent energies: W (the total invariant energy of the colliding particles), E_1 and E_2 (the energies of the scattered protons). So, all the dynamics of the considered process is included in the amplitude g, but the exact form (2) of the spin structure of the matrix element results from a generalized quantum-mechanical kinematics.

The Pauli matrix σ_y, in the parametrization (2), ensures the correct transformation properties of the corresponding two-component spinor products, relative to rotation.

The presence of a single amplitude in (2) implies that the spin directions of all the protons are fixed, with definite relative angles and fixed modules. In other words, all polarization phenomena for $p + p \to p + p + S^0$ at threshold can be predicted without knowing the amplitude g, *i.e. in a model-independent way.* Moreover, these polarization effects are the same for any scalar meson: σ, f_0 or a_0^0. However, the absolute value of the cross-section, which depends on $|g^2|$, is different for different scalar mesons.

All T-odd polarization observables (*i.e.* one-spin and three-spin polarization correlations) are identically zero. The dependence of the cross-section on the polarizations $\mathbf{P}_1$ and $\mathbf{P}_2$ of the colliding protons can be written as

$$\frac{\mathrm{d}\sigma}{\mathrm{d}\omega}(\mathbf{P}_1, \mathbf{P}_2) = \left(\frac{\mathrm{d}\sigma}{\mathrm{d}\omega}\right)_0 (1 - \mathbf{P}_1 \cdot \mathbf{P}_2)\,,$$

(typical for the singlet pp interaction), where $\mathrm{d}\omega$ is the phase space volume element for the three-particles final state and $(\mathrm{d}\sigma/\mathrm{d}\omega)_0$ is the differential cross-section with all unpolarized protons in initial and final states.

All polarization transfer coefficients, characterizing the dependence of the polarization of any final proton on the polarization of the initial proton, vanish also.

The situation is very different in case of np collisions, $n + p \to n + p + S^0$, in the threshold region, where there are three allowed transitions:

$$S_\mathrm{i} = 0,\ \ell = 0 \ \to\ j^P = 0^+ \to S_\mathrm{f} = 0,$$

$$S_\mathrm{i} = 1,\ \ell = 0 \ \to\ j^P = 1^+ \to S_\mathrm{f} = 1,$$

$$S_\mathrm{i} = 1,\ \ell = 2 \ \to\ j^P = 1^+ \to S_\mathrm{f} = 1.$$

The corresponding matrix element can be written in the following form:

$$\begin{aligned}\mathcal{M}_{np} = {} & g_1(\chi_4^\dagger\sigma_y\tilde{\chi}_3^\dagger)(\tilde{\chi}_2\sigma_y\chi_1)\\ & +g_2\left[\chi_4^\dagger(\sigma_a - \hat{k_a}\sigma\cdot\hat{\mathbf{k}})\sigma_y\tilde{\chi}_3^\dagger\right]\\ & \times\left[\tilde{\chi}_2\sigma_y(\sigma_a - \hat{k_a}\sigma\cdot\hat{\mathbf{k}})\chi_1\right] \qquad (3)\\ & +g_3(\chi_4^\dagger\sigma\cdot\hat{\mathbf{k}}\sigma_y\tilde{\chi}_3^\dagger)(\tilde{\chi}_2\sigma_y\sigma\cdot\hat{\mathbf{k}}\chi_1),\end{aligned}$$

where $\hat{\mathbf{k}}$ is the unit vector along the three-momentum of the initial neutron beam, $\sigma = (\sigma_x, \sigma_y, \sigma_z)$ is the standard set of Pauli matrices, and g_1–g_3 are the partial amplitudes for the np interaction. Due to the isotopic invariance of the strong interaction the following relation holds:

$$g_1 = \frac{1}{2}g, \qquad (4)$$

i.e. the triplet-triplet amplitudes g_2 and g_3 are present only in np collisions. Therefore polarization phenomena in $n + p \to n + p + S^0$ collisions are more complicated than in pp collisions. There is no universality here, polarization phenomena are different for the different scalar mesons. There is, however one general feature: all one-spin observables vanish, for $n + p \to n + p + S^0$, in particular the T-odd polarization of the final nucleons, emitted in the collisions of unpolarized nucleons and the analyzing powers in $\vec{n} + p$ or $n + \vec{p}$ collisions.

The ($\mathbf{P}_1$, $\mathbf{P}_2$)-dependence of the differential cross-section for $\vec{n} + \vec{p}$ collisions can be written in the following general form, which is correct near threshold:

$$\frac{\mathrm{d}\sigma}{\mathrm{d}\omega}(\mathbf{P}_1, \mathbf{P}_2) = \left(\frac{\mathrm{d}\sigma}{\mathrm{d}\omega}\right)_0 \left(1 + \mathcal{A}_1\mathbf{P}_1\cdot\mathbf{P}_2 + \mathcal{A}_2\hat{\mathbf{k}}\cdot\mathbf{P}_1\hat{\mathbf{k}}\cdot\mathbf{P}_2\right), \qquad (5)$$

where the real spin correlation coefficients $\mathcal{A}_1$ and $\mathcal{A}_2$ are determined by the following formulas (in terms of the partial threshold amplitudes g_i, $i = 1$–3):

$$\begin{aligned}\mathcal{A}_1\left(\frac{\mathrm{d}\sigma}{\mathrm{d}\omega}\right)_0 &= -|g_1|^2 + |g_3|^2,\\ \mathcal{A}_2\left(\frac{\mathrm{d}\sigma}{\mathrm{d}\omega}\right)_0 &= 2(|g_2|^2 - |g_3|^2). \qquad (6)\end{aligned}$$

The amplitudes g_i are normalized in such way that:

$$\left(\frac{\mathrm{d}\sigma}{\mathrm{d}\omega}\right)_0 = |g_1|^2 + 2|g_2|^2 + |g_3|^2, \qquad (7)$$

where $(\mathrm{d}\sigma/\mathrm{d}\omega)_0$ is the differential cross-section with unpolarized particles. So, from eqs. (6) and (7) one can find:

$$\begin{aligned}4|g_1|^2 &= (1 - 3\mathcal{A}_1 - \mathcal{A}_2)\left(\frac{\mathrm{d}\sigma}{\mathrm{d}\omega}\right)_0,\\ 4|g_2|^2 &= (1 + \mathcal{A}_1 + \mathcal{A}_2)\left(\frac{\mathrm{d}\sigma}{\mathrm{d}\omega}\right)_0, \qquad (8)\\ 4|g_3|^2 &= (1 + \mathcal{A}_1 - \mathcal{A}_2)\left(\frac{\mathrm{d}\sigma}{\mathrm{d}\omega}\right)_0,\end{aligned}$$

which shows that the moduli of the three threshold amplitudes for $n + p \to n + p + S^0$ can be determined by the measurement of $\mathcal{A}_1$, $\mathcal{A}_2$, and $(\mathrm{d}\sigma/\mathrm{d}\omega)_0$. Taking into account the isotopic relation (4), one obtains

$$\mathcal{R} = \frac{(\mathrm{d}\sigma_{np}/\mathrm{d}\omega)_0}{(\mathrm{d}\sigma_{pp}/\mathrm{d}\omega)_0} = (1 - 3\mathcal{A}_1 - \mathcal{A}_2)^{-1}.$$

The dependence of the polarization $\mathbf{P}_3$ of the final neutron on the polarization $\mathbf{P}_1$ of the initial neutron can be parametrized as

$$\mathbf{P}_3 = p_1\mathbf{P}_1 + p_2\hat{\mathbf{k}}(\hat{\mathbf{k}}\cdot\mathbf{P}_1), \qquad (9)$$

where p_1 and p_2 are the spin transfer coefficients, which can be expressed in terms of the partial amplitudes g_i:

$$\begin{aligned}p_1 &= -\frac{2\mathcal{R}eg_2(g_1 - g_3)^*}{|g_1|^2 + 2|g_2|^2 + |g_3|^2},\\ p_2 &= \frac{2|g_2|^2 - 2\mathcal{R}e\left[g_1g_3^* - g_2(g_1 - g_3)^*\right]}{|g_1|^2 + 2|g_2|^2 + |g_3|^2}. \qquad (10)\end{aligned}$$

The dependence of the polarization $\mathbf{P}_4$ of the final proton on the polarization $\mathbf{P}_1$ of the initial neutron can be also be parametrized in terms of two real coefficients:

$$\mathbf{P}_4 = p_3\mathbf{P}_1 + p_4\hat{\mathbf{k}}(\hat{\mathbf{k}}\cdot\mathbf{P}_1) \qquad (11)$$

with the following formulas for p_3 and p_4:

$$\begin{aligned}p_3 &= \frac{2\mathcal{R}eg_2(g_1 + g_3)^*}{|g_1|^2 + 2|g_2|^2 + |g_3|^2},\\ p_4 &= \frac{2|g_2|^2 + 2\mathcal{R}e\left[g_1g_3^* - g_2(g_1 + g_3)^*\right]}{|g_1|^2 + 2|g_2|^2 + |g_3|^2}. \qquad (12)\end{aligned}$$

Comparing eqs. (6), (7), (10), and (12), one can find the following relation between these polarization observables:

$$p_1 + p_2 + p_3 + p_4 = 1 + \mathcal{A}_1 + \mathcal{A}_2, \qquad (13)$$

which has to be verified by any model describing this process.

Note that the isovector a_0-meson can be produced in the following processes of the NN interaction:

$$\begin{aligned}&p + p \to p + p + a_0^0,\\ &p + p \to n + p + a_0^+,\\ &n + p \to p + p + a_0^-,\\ &n + p \to n + p + a_0^0.\end{aligned}$$

It is possible to show that the production of the charged $a_0^\pm$-mesons in the near-threshold regime is characterized by a single amplitude, with the spin structure as in eq. (2), where the following relations hold:

$$g(pp \to npa_0^+) = -g(np \to ppa_0^-) = \frac{1}{\sqrt{2}}g(pp \to ppa_0^0).$$

Therefore the previous statements on polarization phenomena for $p + p \to p + p + S^0$ apply also to the production of the charged $a_0^\pm$-mesons.

3 The dynamics for the t-channel

The standard dynamics for different processes of meson production in NN collisions, $N + N \rightarrow N + N + P$, $N + N \rightarrow N + N + S$, and $N + N \rightarrow N + N + V$, (where P, S, and V denote pseudoscalar, scalar and vector mesons, respectively) is based on the consideration of mesonic exchanges in the t-channel, such as π, η, σ, a_0, ρ, ω, etc. In such approach one has to know the meson-nucleon coupling constants, PNN, SNN, and VNN and the amplitudes of different subprocesses, such as

$$\begin{aligned} &P^* + N \rightarrow N + S, \\ &S^* + N \rightarrow N + S, \\ &V^* + N \rightarrow N + S, \end{aligned} \tag{14}$$

where the exponent * denotes virtual mesons with space-like four-momenta. In principle some information exists on the coupling constants, but the threshold amplitudes for the processes (14) are poorly known, in particular for those processes that cannot be directly studied. Therefore model calculations have to be done, in order to find these amplitudes. In case of complex amplitudes not only the absolute values are important, but also the relative signs and phases.

In this section we analyze different t-channel exchanges for the processes of scalar-meson production in NN collisions, and give, when it is possible, model-independent predictions. In other words, we will find expressions for the polarization observables in $n + p \rightarrow n + p + S^0$, which depend only on the quantum numbers, spin and parity $\mathcal{J}^P$, and isospin $\mathcal{I}$, of the exchanged meson, but not on the corresponding coupling constants, hadronic form factors and threshold amplitudes. For this aim, let us consider the spin structure of the matrix element for different exchanged particles.

3.1 Scalar and pseudoscalar exchange

Taking into account the identity of initial and final protons in $p+p \rightarrow p+p+S^0$, the σ exchange here is characterized by four different t-channel diagrams (fig. 1). Each diagram has a different spin structure, where the order of the two-component spinors χ_i, $i = 1$–4 is different. Only the sum of all these diagrams, which satisfies the Pauli principle for the initial and final protons, generates the correct spin structure (2), with a single amplitude g. In threshold conditions each propagator for the considered diagrams is the same, and can be written as $\dfrac{1}{t - m_\sigma^2} = -\dfrac{1}{mm_s + m_\sigma^2}$, where t is the momentum transfer squared between the initial and final nucleons, m, m_σ, and m_s are the masses of the nucleon, of the virtual σ-meson, and of the produced scalar meson, respectively. Such equality is correct at the reaction threshold, and it follows from the assumption of S-wave production of final particles. The difference in these propagators, which appears far from threshold, generates P- and higher waves of produced particles.

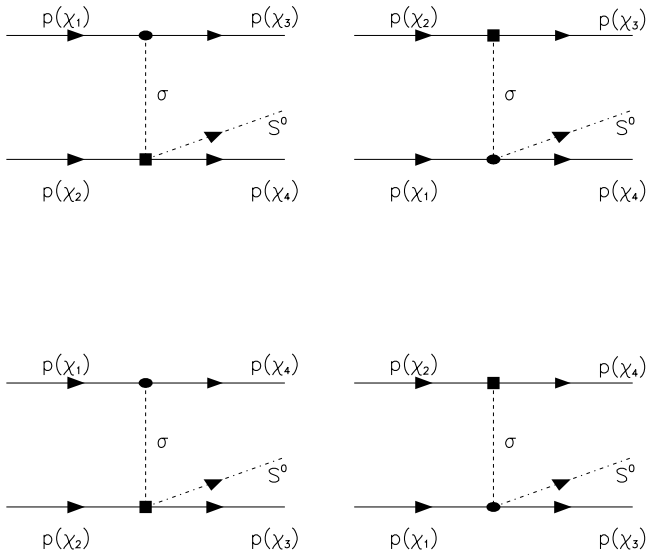

Fig. 1. Feynman diagrams for σ exchange, for $p + p \rightarrow p + p + S^0$, where $p(\chi_i)$, $i = 1$–4, means that the corresponding proton (in initial or final state) is described by the 2-component spinor χ_i.

In order to find the partial amplitudes g_i, corresponding to the different t-channel exchanges, it is necessary to apply the Fierz transformation, in its two-component form, to the spinor constructions which appear in the matrix elements for different t-channel exchanges as in figs. 2 (3) for σ (π) exchanges, respectively. The corresponding results are shown in table 1, where we use the following notations:

$$\mathcal{A}_M = \frac{g_{MNN}}{t - m_M^2} \mathcal{N} F_M(t) A(M^* N \rightarrow NS) \mathcal{P}, \tag{15}$$

where g_{MNN} [$F_M(t)$] is the coupling constant [form factor] for the vertex MNN, with $M = \sigma$, η π or a_0, $A(M^*N \rightarrow NS)$ is the threshold amplitude for the subprocess $M^* + N \rightarrow S + N$, $\mathcal{N} = 2m(E + m)$ is the normalization factor, related to the transformation from four-component Dirac spinors to two-component Pauli spinors, with $\mathcal{P} = 1$ $\left[\sqrt{m_s/(4m + m_s)}\right]$ for positive (negative) P-parity of the M-meson.

In table 2 we report the values of the analyzing powers, of the spin transfer coefficients and of the isotopic ratio, in order to show the sensitivity of these quantities to the quantum numbers of the possible t-channel exchanges. These predictions are independent of the details of the considered exchange, such as the value of the constant g_{MNN}, the amplitude $A(MN \rightarrow NS^0)$, and the choice of the form factor $F_M(t)$. One can see that the polarization transfer coefficients, characterizing a change of neutron polarization, are very sensitive to the quantum number of the isoscalar exchange in the t-channel; other polarization observables, such as $\mathcal{A}_1$ p_3 and p_4 vanish for both exchanges $\mathcal{J}^P = 0^+$ and $\mathcal{J}^P = 0^-$, $\mathcal{A}_2 = 0$ in all the cases considered here.

Table 1. Partial amplitudes for $N + N \to N + N + S^0$ for different spin, parity and isotopic spin of the exchanged meson.

$\mathcal{J}^P, \mathcal{I}$	$g_1(np \to npS^0)$	$g_2(np \to npS^0)$	$g_3(np \to npS^0)$	$g(pp \to ppS^0)$
$0^+, \mathcal{I} = 0$	$-A_\sigma$	A_σ	A_σ	$-2A_\sigma$
$0^-, \mathcal{I} = 0$	$-A_\eta$	$-A_\eta$	A_η	$-2A_\eta$
$0^-, \mathcal{I} = 1$	A_π	$-3A_\pi$	$3A_\pi$	$2A_\pi$
$0^+, \mathcal{I} = 1$	A_a	$3A_a$	$3A_a$	$2A_a$

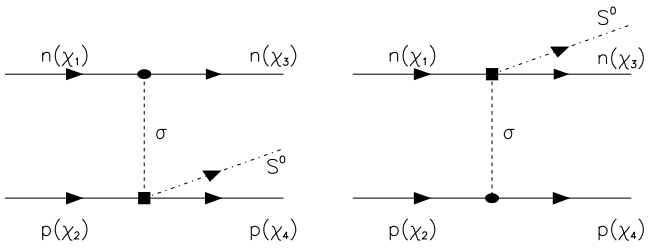

Fig. 2. Feynman diagrams for σ exchange for $n+p \to n+p+S^0$. Notations as in fig. 1.

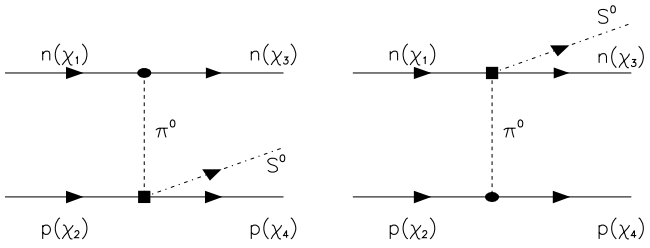

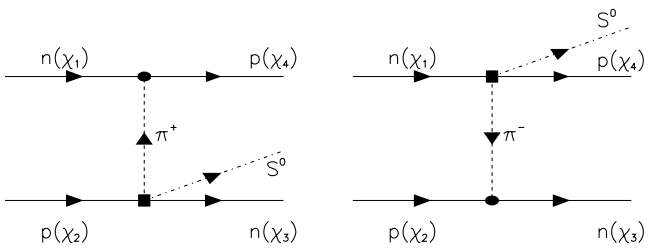

Fig. 3. Feynman diagrams for π exchange for $n+p \to n+p+S^0$. Notations as in fig. 1.

Table 2. Polarization phenomena for $n + p \to n + p + S^0$ for different spin, parity and isotopic spin of the exchanged meson.

$\mathcal{J}^P, \mathcal{I}$	A_1	A_2	p_1	p_2	p_3	p_4	$\mathcal{R}$
$0^+, \mathcal{I} = 0$	0	0	1	0	0	0	2
$0^-, \mathcal{I} = 0$	0	0	-1	2	0	0	2
$0^-, \mathcal{I} = 1$	2/7	0	$-3/7$	6/7	$-6/7$	12/7	14
$0^+, \mathcal{I} = 1$	2/7	0	3/7	0	6/7	0	14

Another interesting result concerns the large difference in cross-section, for *pp* and *np* interactions: $\mathcal{R}_\pi = 14$, *i.e.* for the scalar-meson production (in the NN interaction) we have a large isotopic dependence.

3.2 Vector-meson exchange

This case has to be analyzed separately. The starting point is the following relativistic invariant expression for the matrix element, corresponding to V exchange ($V = \omega$- or ρ-meson), in the process $N + N \to N + N + S^0$:

$$\mathcal{M}_V = \mathcal{J}_\mu^{(1)} \left(-g_{\mu\nu} + \frac{Q_\mu Q_\nu}{m_V^2} \right) \mathcal{J}_\nu^{(2)} \frac{1}{t - m_V^2}, \qquad (16)$$

where

$$\mathcal{J}_\mu^{(1)} = g_{VNN} \overline{u} \left(\gamma_\mu - \kappa_V \frac{\sigma_{\mu\nu} Q_\nu}{2m} \right) u$$

is the vector current for the VNN-vertex, g_{VNN} is the vector coupling constant for this vertex, κ_V is the ratio of vector and tensor couplings, $\mathcal{J}_\nu^{(2)}$ is the vector current corresponding to the process $V^* + N \to N + S^0$, Q is the four-momentum transfer. Taking into account the currents conservation: $Q \cdot \vec{\mathcal{J}}^{(1)} = Q \cdot \vec{\mathcal{J}}^{(2)} = 0$, one can rewrite the matrix element $\mathcal{M}_V$ in terms of the space components of these currents only:

$$\mathcal{M}_V = \frac{1}{t - m_V^2} \left(\vec{\mathcal{J}}_{\rm T}^{(1)} \cdot \vec{\mathcal{J}}_{\rm T}^{(2)} + \frac{4m^2}{t} \mathcal{J}_{\rm L}^{(1)} \vec{\mathcal{J}}_{\rm L}^{(2)} \right), \qquad (17)$$

where $\vec{\mathcal{J}}_{\rm T,L}^{(i)}$, $i = 1, 2$ are the transversal and longitudinal components of the corresponding currents relative to the direction $\mathbf{k}$.

The current $\vec{\mathcal{J}}^{(1)}$ has the following form, at the reaction threshold of $N + N \to N + N + S^0$:

$$\vec{\mathcal{J}}^{(1)} = \chi^\dagger \left(i G_M \sigma \times \hat{\mathbf{k}} + G_E \hat{\mathbf{k}} \right) \chi \frac{|\mathbf{k}|}{E + m},$$

where

$$G_M(t) = g_{VNN}(1 + \kappa_V) F_{VNN}(t),$$

$$G_E(t) = g_{VNN} \left(1 + \kappa_V \frac{t}{4m^2} \right) F_{VNN}(t)$$

and $F_{VNN}(t)$ is a phenomenological form factor for the VNN-vertex.

The current $\vec{\mathcal{J}}^{(2)}$ describes two possible threshold partial transitions for the subprocess $V^* + N \to N + S^0$ (V^* is the virtual V-meson):

$$\ell_V = 1, \ S = 1/2 \ \to \ \mathcal{J}^P = 1/2^+,$$

$$\ell_V = 1, \ S = 3/2 \ \to \ \mathcal{J}^P = 3/2^+,$$

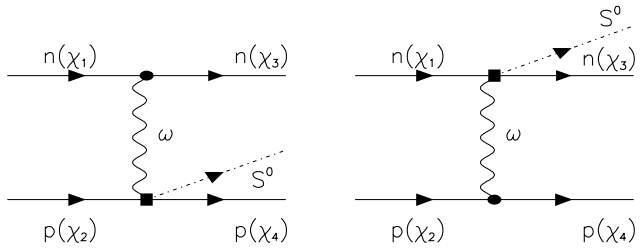

Fig. 4. ω exchange for the process $n+p \to n+p+S^0$. Notations as in fig. 1.

where ℓ_V is the orbital momentum of the V-meson, and S is the total spin of the VN-system. Therefore, the general parametrization of the current $\vec{\mathcal{J}}^{(2)}$ can be written as follows:

$$\vec{\mathcal{J}}^{(2)} = \chi^\dagger \left(-ih_{1V}\sigma \times \hat{\mathbf{k}} + h_{2V}\hat{\mathbf{k}}\right)\chi,$$

where h_{1V} and h_{2V} are the corresponding partial amplitudes.

The matrix element $\mathcal{M}_\omega$, for the isoscalar ω exchange, corresponding to the two possible diagrams for the process $n+p \to n+p+S^0$, fig. 4, can be written as follows:

$$\begin{aligned}
\mathcal{M}_\omega &= \mathcal{M}_{1\omega} + \mathcal{M}_{2\omega},\\
\mathcal{M}_{1\omega} &= \frac{1}{t-m_\omega^2}\left\{G_{E\omega}h_{2\omega}\frac{4m^2}{t}(\chi_3^\dagger\mathcal{I}\chi_1)(\chi_4^\dagger\mathcal{I}\chi_2)\right.\\
&\quad \times G_{M\omega}h_{1\omega}\left[\chi_3^\dagger(\sigma\times\hat{\mathbf{k}})_a\chi_1\right]\\
&\quad \left.\times\left[\chi_4^\dagger(\sigma\times\hat{\mathbf{k}})_a\chi_2\right]\right\}\frac{|\mathbf{k}|}{E+m},\\
\mathcal{M}_{2\omega} &= \mathcal{M}_{1\omega}(\chi_1 \leftrightarrow \chi_2,\ \chi_3 \leftrightarrow \chi_4).
\end{aligned} \tag{18}$$

Applying the Fierz transformation to the matrix element (18), one can find the following formulas for the ω contribution to the partial amplitudes $g_{i\omega}$, $i=1$–3:

$$\begin{aligned}
g_{1\omega} &= \left(G_{E\omega}h_{2\omega}\frac{4m^2}{t} - 2G_{M\omega}h_{1\omega}\right)\frac{1}{t-m_\omega^2}\frac{|\mathbf{k}|}{E+m},\\
g_{2\omega} &= -G_{E\omega}h_{2\omega}\frac{4m^2}{t}\frac{1}{t-m_\omega^2}\frac{|\mathbf{k}|}{E+m},\\
g_{3\omega} &= -\left(G_{E\omega}h_{2\omega}\frac{4m^2}{t} + 2G_{M\omega}h_{1\omega}\right)\frac{1}{t-m_\omega^2}\frac{|\mathbf{k}|}{E+m}.
\end{aligned} \tag{19}$$

The ρ exchange mechanism for $n+p \to n+p+S^0$, ($S^0=\sigma$ or f_0), is described by four different Feynman diagrams, corresponding to neutral and charged vector mesons. Taking into account the standard isotopic relations between the coupling constants $g_{\rho NN}$ for the different vertices ρNN , and among the amplitudes $h_{i\rho}$ for the subprocesses $\rho+N \to N+S^0$, one can find the following expressions for the ρ contribution to the partial amplitudes $g_{i\rho}$, $i=1$–3:

$$\begin{aligned}
g_{1\rho} &= -\left(G_{E\rho}h_{2\rho}\frac{4m^2}{t} - 2G_{M\rho}h_{1\rho}\right)\frac{1}{t-m_\rho^2}\frac{|\mathbf{k}|}{E+m},\\
g_{2\rho} &= -3G_{E\rho}h_{2\rho}\frac{4m^2}{t}\frac{1}{t-m_\rho^2}\frac{|\mathbf{k}|}{E+m},\\
g_{3\rho} &= -3\left(G_{E\rho}h_{2\rho}\frac{4m^2}{t} + 2G_{M\rho}h_{1\rho}\right)\frac{1}{t-m_\rho^2}\frac{|\mathbf{k}|}{E+m},
\end{aligned} \tag{20}$$

where

$$G_{E\rho} = g_{\rho NN}\left(1+\kappa_\rho\frac{t}{4m^2}\right)F_{\rho NN}(t),$$

$$G_{M\rho} = g_{\rho NN}\left(1+\kappa_\rho\right)F_{\rho NN}(t).$$

For the numerical estimations we will assume that $F_{\rho NN}(t) = F_{\omega NN}(t)$.

3.3 Correlation of spin and isospin structures for the threshold regime

Combining the contributions derived above, one can find for the threshold amplitudes g_i the following expressions:

$$\begin{aligned}
g_1(np \to npS^0) &= -A_\sigma + A_a - A_\eta + A_\pi,\\
g_2(np \to npS^0) &= A_\sigma + 3A_a - A_\eta - 3A_\pi,\\
g_3(np \to npS^0) &= A_\sigma + 3A_a + A_\eta + 3A_\pi,\\
g(pp \to ppS^0) &= 2g_1(np \to npS^0).
\end{aligned} \tag{21}$$

The S-channel parametrization of the spin structure for the threshold matrix elements allows (after applying the Fierz transformation) to unify different t-channel contributions —with different $\mathcal{J}^P$— in a universal and transparent form, which is well adapted to the analysis of the sensitivity of the polarization phenomena to the quantum numbers of the t-channel meson. Such unification allows to simplify the calculations: we can express the matrix element for any exchange in terms of three amplitudes only, whereas, for example, a model with $\eta+\pi+\sigma+a$ contains $2+4+2+4=12$ different Feynman diagrams with different spin structures. All these twelve contributions to the total matrix elements, in general, interfere, so it is in principle necessary to calculate $12\times 12 = 144$ terms, instead of $3\times 3 = 9$ terms. Moreover, these nine terms are the same for any model, whereas, for example, adding vector exchanges will increase essentially the number of t contributions. Another advantage of the $t \to s$ Fierz transformation is the explicit dependence of the observables on a definite combination of coupling constants, hadronic form factors and elementary amplitudes. This helps in finding out which contributions play the most important role in the t-channel dynamics, and gives a feedback on the coupling constants by comparison with the experimental data.

Another important property of the partial amplitudes g_i for np processes, eq. (21), concerns a strong correlation of the spin and isospin structure of the matrix element

in the threshold region. The amplitudes $g_2(np \to npS^0)$ and $g_3(np \to npS^0)$, describing the np interaction in the isotopic singlet state, are in general different, even in case of a definite isospin in the t-channel, if the P-parity of the t-channel is not fixed. However, for definite $\mathcal{J}^P$ exchanges, we have

$$g_2(np \to npS^0) = g_3(np \to npS^0), \text{ if } \mathcal{J}^P = 0^+,$$
$$g_2(np \to npS^0) = -g_3(np \to npS^0), \text{ if } \mathcal{J}^P = 0^-,$$
$$\mathcal{I} = 0 \text{ or } \mathcal{I} = 1. \quad (22)$$

The relations (22) hold also for any combination of isoscalar and isovector exchanges, but only in the case of $\mathcal{J} = 0$. But for vector exchange, eqs. (19) and (20), the relations (22) do not hold any longer. It is another example of the strong correlation of spin and isospin structure for threshold scalar-meson production.

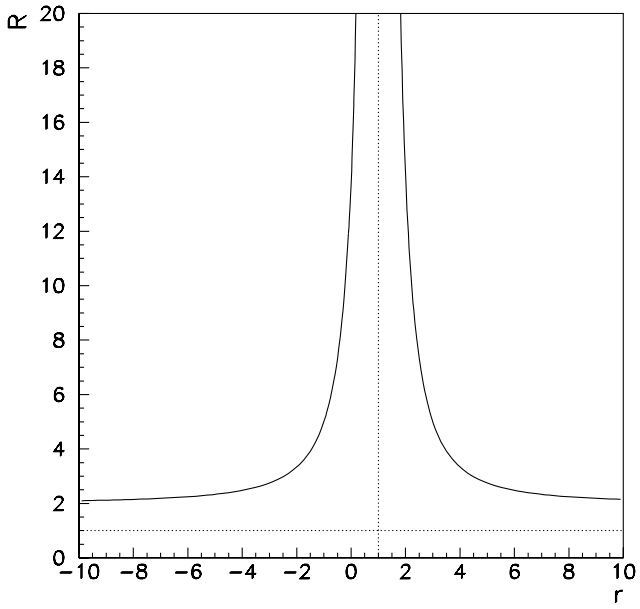

Fig. 5. Dependence of R on r, see eq. (24).

4 A possible model for N + N → N + N + S⁰

In the previous section, we analyzed the predictions for the polarization observables in the simplest case of t-channel exchange with definite quantum numbers. All polarization effects depend on these quantum numbers and are independent of the dynamics of the corresponding subprocesses. Such analysis allows a quick estimation of the relative role of the different exchanges, but it may be an oversimplified picture. Even the combination of any pair of the above-considered contributions changes essentially the predictions. This is shown in this section, where we analyze in detail a model for $N + N \to N + N + S^0$, based on $\sigma + \pi$ exchange. In order to justify such model, let us mention that the η contribution can be neglected, in (21), due to the fact that the coupling constant $g_{\eta NN}$ is presently poorly known, the allowed range being 1–7 [46–49]. Concerning the a_0 exchange, both the ingredients of such contribution, the coupling constant g_{aNN} and the amplitude $A(aN \to NS^0)$ are presently not well known. The mass of the a_0-meson is larger in comparison with the pion mass. In any case, the $\sigma + \pi$ model can be considered a realistic starting point for the analysis, containing the exchange of mesons with different P-parities and isospin. As a result, all three partial amplitudes g_i, are different:

$$\begin{aligned} g_1(np \to npS^0) &= A_\pi(1 - r), \\ g_2(np \to npS^0) &= A_\pi(-3 + r), \\ g_3(np \to npS^0) &= A_\pi(3 + r), \\ g(pp \to ppS^0) &= 2A_\pi(1 - r), \end{aligned} \quad (23)$$

where r is the ratio of the corresponding contributions:

$$r = \frac{g_{\sigma NN}}{g_{\pi NN}} \left(\frac{t - m_\pi^2}{t - m_\sigma^2} \right) \frac{A(\sigma^* N \to NS^0)}{A(\pi^* N \to NS^0)} \times \sqrt{\left(1 + 4\frac{m}{m_s}\right)} \frac{F_\sigma(t)}{F_\pi(t)}.$$

One can see that all the physics of this model (with eight different Feynman diagrams) is contained in a single parameter r, which is basically the ratio of the coupling constants and the elementary amplitudes. In the general case, the ratio r is a complex parameter, which depends on the excitation energy of the produced NNS-system. Therefore the polarization phenomena for the process $n + p \to n + p + S^0$ and the ratio of cross-section for np and pp collisions, can be expressed in terms of two parameters $|r|^2$ and $\mathcal{R}er$:

$$\mathcal{R} = \frac{\sigma(np \to npS^0)}{\sigma(pp \to ppS^0)} = 2\frac{7 - 2\mathcal{R}er + |r|^2}{1 - 2\mathcal{R}er + |r|^2} = 2\left(7 - 6\frac{|r|^2 - 2\mathcal{R}er}{1 - 2\mathcal{R}er + |r|^2}\right). \quad (24)$$

The coefficients $\mathcal{A}_1$ and $\mathcal{A}_2$, which characterize the polarized $\vec{n}\vec{p}$ collisions, can be written as follows:

$$\mathcal{A}_1 = 2\frac{1 + \mathcal{R}er}{7 - 2\mathcal{R}er + |r|^2}, \ \mathcal{A}_2 = \frac{3\mathcal{R}er}{7 - 2\mathcal{R}er + |r|^2}. \quad (25)$$

The ratio r can be found in the framework of a model for the elementary subprocesses $\pi^*(\sigma^*) + N \to N + S^0$, under several assumptions concerning coupling constants, cut-off parameters, form factors and reaction mechanism, as well. To avoid the uncertainties related to these choices, we assume for simplicity that r is real. This is the case, for example, of the effective Lagrangian approach, which gives real amplitudes and, therefore, real values for the ratio r. Another possibility is the saturation of the $A(\sigma^* N \to NS^0)$ and $A(\pi^* N \to NS^0)$ amplitudes by a single nucleon resonance (with $\mathcal{J}^P = 1/2^+$). Such mechanism produces complex amplitudes with zero relative phase, and r is a real parameter, too.

In this case we can predict the r-dependence of $\mathcal{R}$, $\mathcal{A}_1$, and $\mathcal{A}_2$ (figs. 5-7). The ratio R of the corresponding cross-sections can be very large in the region $r \simeq 1$ (fig. 5). The

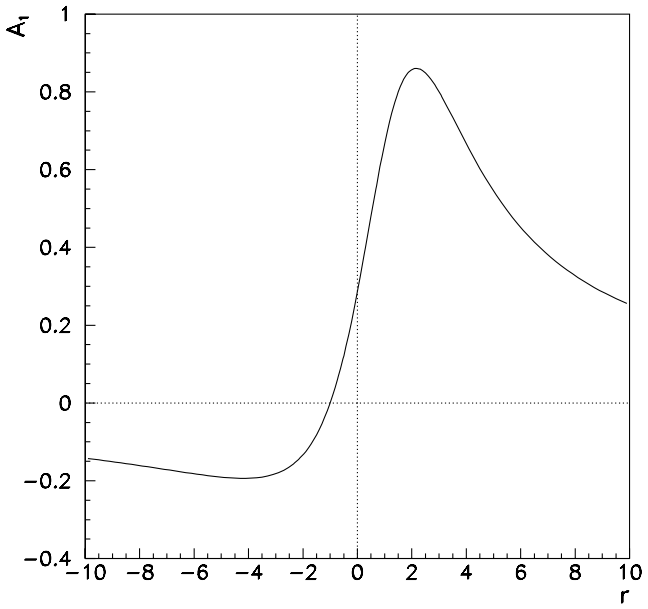

Fig. 6. Dependence of $\mathcal{A}_1$ on r, see eq. (25).

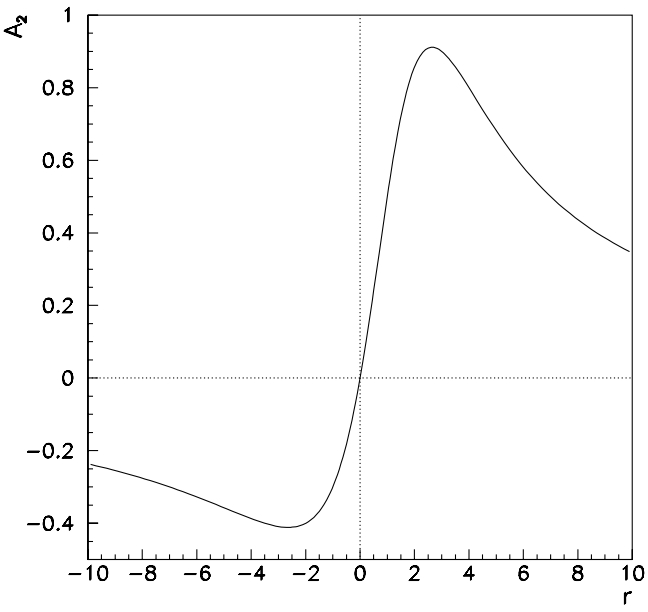

Fig. 7. Dependence of $\mathcal{A}_2$ on r, see eq. (25).

experimental determination of R will allow to find two solutions for r:

$$r_{\pm} = 1 \pm 2\sqrt{\frac{3}{R-2}}.$$

The function $A_1(r)$ has two extrema: the maximum at $r = -1 + \sqrt{10}$, where $A_1^{\max} = (2 + \sqrt{10})/\sqrt{6}$ and a minimum at $r = -1 - \sqrt{10}$, where $A_1^{\min} = (2 - \sqrt{10})/\sqrt{6}$ (fig. 6).

The function $A_2(r)$ has a similar behavior, with the maximum at $r = +\sqrt{7}$, where $A_2^{\max} = (1 + \sqrt{7})/4$ and a minimum at $r = -\sqrt{7}$, where $A_2^{\min} = (12 - \sqrt{7})/4$ (fig. 7).

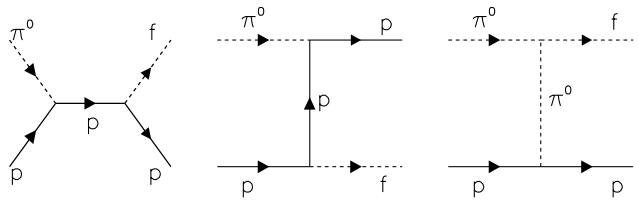

Fig. 8. Pole diagrams for the $\pi^0 + p \to p + f$ subprocess.

The suggested model, based on $\pi + \sigma$ exchange, is certainly an oversimplified description for the process $N + N \to N + N + S$ in the threshold region. Nevertheless this model is an example to illustrate the power of the present formalism, which allows to combine the corresponding coupling constants and the threshold amplitudes in a reduced number of physical parameters. This model can be easily extended to the vector-meson exchange (see sect. 6).

5 Analysis of the subprocesses $\mathbf{M + N \to N + S^0}$

For the calculation of the partial threshold amplitudes for the processes $N + N \to N + N + S$ important ingredients are the partial amplitudes for all the subprocesses $M^* + N \to N + S^0$, where M^* is a virtual meson, $M^* = \pi$, η, f, a_0, ω and ρ^0.

In the framework of the effective Lagrangian approach, one can consider the simplest pole diagrams in s-, t-, and u-channels, in the kinematical conditions of threshold production of scalar mesons in NN collisions. The Mandelstam variables s, t, and u, for any subprocess $M^*(k) + N(p_1) \to N(p_2) + S^0(q)$ (where the four-momentum of each particle is indicated in brackets), are written as

$$\begin{aligned} &s = (k + p_1)^2 = (m_s + m)^2,\ t = (p_1 - p_2)^2 = -m_s m, \\ &u = (p_1 - q)^2 = m^2 - 2mm_s, \end{aligned} \tag{26}$$

and take definite values. Moreover, in these kinematical conditions $k^2 = -m_s m$. As an example, we consider here the production of the isoscalar $f_0(980)$-meson, $m_s \to m_f$.

5.1 The process $\pi^0 + \mathbf{p} \to \mathbf{p} + \mathbf{f}$

The matrix element, corresponding to the diagrams illustrated in fig. 8, can be written as follows:

$$\begin{aligned} \mathcal{M}_\pi &= \mathcal{M}_s + \mathcal{M}_u + \mathcal{M}_t, \\ \mathcal{M}_s &= \frac{g_{\pi NN} g_{fNN}}{s - m^2} \overline{u}(p_2)(\hat{p_1} + \hat{q} + m)\gamma_5 u(p_1), \\ \mathcal{M}_u &= \frac{g_{\pi NN} g_{fNN}}{u - m^2} \overline{u}(p_2)\gamma_5(\hat{p_2} - \hat{q} + m)u(p_1), \\ \mathcal{M}_t &= \frac{g_{\pi NN} g_{\pi\pi f}}{t - m_\pi^2} m_f \overline{u}(p_2)\gamma_5 u(p_1), \end{aligned} \tag{27}$$

where g_{fNN} is the coupling constant for the fNN-vertex and $g_{\pi\pi f}$ is the coupling constant for the vertex $f_0 \to$

$(\pi^+\pi^-)+(\pi^0\pi^0)$. In such normalization, the decay width for $f_0 \to \pi\pi$ can be written as follows:

$$\Gamma(f_0 \to \pi\pi) = \frac{3}{32\pi} g^2_{\pi\pi f} m_f \sqrt{1-\frac{4m^2_\pi}{m^2_f}}. \qquad (28)$$

The matrix element (27) generates the following expression for the threshold amplitude $\mathcal{A}(\pi N \to Nf)$:

$$\begin{aligned}
&\mathcal{A}(\pi^* N \to Nf) = \frac{g_{\pi NN} g_{fNN}}{E+m} \\
&\times \left[(W+m)\left(\frac{1}{s-m^2}+\frac{1}{u-m^2}\right)+\frac{m_s}{t-m^2_\pi}\frac{g_{\pi\pi f}}{g_{fNN}}\right] \\
&= g_{\pi NN} g_{fNN} \frac{|\mathbf{k}|}{2m(E+m)}\left(-1+\frac{2mm_f}{t-m^2_\pi}\frac{g_{\pi\pi f}}{g_{fNN}}\right), \\
&s = W^2. \qquad (29)
\end{aligned}$$

One can see, that for the pseudoscalar πNN interaction, there is a compensation of the s and u contributions. The numerical value of the amplitude $\mathcal{A}(\pi^* N \to Nf)$ depends on the relative sign of the coupling constants $g_{\pi\pi f}$ and $g_{\pi NN}$. The effects of the form factors will be discussed later.

Following a similar procedure, we can write the following expression for the threshold amplitude of $\eta^* + N \to N + f$:

$$\begin{aligned}
\mathcal{A}(\eta^* N \to Nf) &= g_{\eta NN} g_{fNN} \frac{|\mathbf{k}|}{2m(E+m)} \\
&\times \left(-1+\frac{2mm_f}{t-m^2_\eta}\frac{g_{\eta\eta f}}{g_{fNN}}\right), \qquad (30)
\end{aligned}$$

where $g_{\eta\eta f}$ is the coupling constant for the $f\eta\eta$-vertex, which can be related to $g_{\pi\pi f}$ through the $SU(3)$ symmetry.

5.2 The process $f^* + N \to N + f$

The matrix element, corresponding to the diagrams illustrated in fig. 8, can be written as follows:

$$\begin{aligned}
\mathcal{M}_f &= \mathcal{M}_s + \mathcal{M}_u + \mathcal{M}_t, \\
\mathcal{M}_s &= \frac{g^2_{fNN}}{s-m^2}\overline{u}(p_2)(\hat{p_1}+\hat{q}+m)u(p_1), \\
\mathcal{M}_u &= \frac{g^2_{fNN}}{u-m^2}\overline{u}(p_2)(\hat{p_2}-\hat{q}+m)u(p_1), \qquad (31) \\
\mathcal{M}_t &= \frac{g_{fNN} g_{fff} m_f}{t-m^2_f}\overline{u}(p_2)u(p_1),
\end{aligned}$$

where g_{fff} is the coupling constant for triple self-interacting f-mesons, m_f is the mass of the f-meson.

The threshold amplitude $\mathcal{A}(f^* N \to Nf)$ can be written in the following form:

$$\begin{aligned}
&\mathcal{A}(f^* N \to NS) = g^2_{fNN} \\
&\times \left(\frac{2m+m_f}{s-m^2}+\frac{2m-m_f}{u-m^2}+\frac{m_f}{t-m^2_f}\frac{g_{fff}}{g_{fNN}}\right) \\
&= g^2_{fNN}\frac{1}{2m}\left(1-\frac{2m}{m+m_f}\frac{g_{fff}}{g_{fNN}}\right), \qquad (32)
\end{aligned}$$

i.e. in the considered approximation there is, again, a partial compensation of the s and u contributions.

5.3 The processes $V^* + N \to N + f$, $V = \omega$ or ϕ

Again we can describe this process in terms of three pole mechanisms, as in fig. 8, ($\pi \to V^*$). Therefore the matrix element can be written in the following relativistic invariant form:

$$\begin{aligned}
\mathcal{M}_V &= \mathcal{M}_s + \mathcal{M}_u + \mathcal{M}_t, \\
\mathcal{M}_s &= \frac{g_{VNN} g_{fNN}}{s-m^2}\overline{u}(p_2)(\hat{p_2}+\hat{q}+m) \\
&\quad \times \left(\hat{U} - \kappa_V \frac{\sigma_{\mu\nu} U_\mu k_\nu}{2m}\right) u(p_1), \\
\mathcal{M}_u &= \frac{g_{VNN} g_{fNN}}{u-m^2}\overline{u}(p_2)\left(\hat{U} - \kappa_V \frac{\sigma_{\mu\nu} U_\mu k_\nu}{2m}\right) \\
&\quad \times(\hat{p_1}-\hat{q}+m)u(p_1), \\
\mathcal{M}_t &= \frac{g_{fVV} g_{VNN} m_f}{t-m^2_f}\overline{u}(p_2)\left[\hat{U} - \kappa_V \frac{\sigma_{\mu\nu} U_\mu (k-q)_\nu}{2m}\right] u(p_1),
\end{aligned} \qquad (33)$$

where $g_{fVV}$is the coupling constant for the fVV-vertex with the following Lagrangian:

$$\mathcal{L}_{fVV} = m_f g_{fVV} f(x) U^\mu(x) U_\mu(x), \qquad (34)$$

and U is the polarization four-vector of the V-meson.

The threshold amplitudes h_{1V} and h_{2V}, which drive the V exchange for scalar-meson production in $N + N \to N + N + f$, can be written as follows (in terms of the corresponding coupling constants):

$$\begin{aligned}
h_{1V} &= g_{VNN} g_{fNN} \frac{|\mathbf{k}|}{E+m}\left\{\frac{1}{m_f}+\frac{W+m}{u-m^2}\right. \\
&\quad + \frac{\kappa_V}{2m}\left(\frac{2m+m_f}{m_f}+\frac{4m^2}{u-m^2}\right) \\
&\quad \left. + \frac{m_f}{t-m^2_V}\frac{g_{fVV}}{g_{fNN}}\left[1+\kappa_V\left(1+\frac{m_f}{2m}\right)\right]\right\} \qquad (35) \\
&= g_{VNN} g_{fNN} \frac{|\mathbf{k}|}{m(4m+m_f)} \\
&\quad \times\left\{-1+\kappa_V+\frac{m^2_f}{t-m^2_V}\frac{g_{fVV}}{g_{fNN}}\left[1+\kappa_V\left(1+\frac{m_f}{2m}\right)\right]\right\},
\end{aligned}$$

$$\begin{aligned}
h_{2V} &= g_{VNN} g_{fNN} \frac{|\mathbf{k}|}{E+m}\left\{(W+m)\left(\frac{1}{s-m^2}\right.\right. \\
&\quad \left.+\frac{1}{u-m^2}\right)+\kappa_V\frac{k_0}{2m}\left(\frac{1}{m_f}+\frac{E+m}{u-m^2}\right) \\
&\quad \left. + \frac{m_f}{t-m^2_V}\frac{g_{fVV}}{g_{fNN}}\left[1+\frac{\kappa_V}{2}\left(1-\frac{m_f}{2m}\right)\right]\right\} \qquad (36) \\
&= -g_{VNN} g_{fNN} \frac{|\mathbf{k}|}{E+m_f}\frac{1}{2m}\left\{1+\kappa_V\frac{m_f}{4m}\right. \\
&\quad \left. - \frac{g_{fVV}}{g_{fNN}}\frac{2mm_f}{t-m^2_V}\left[1-\frac{\kappa_V}{2}\left(1-\frac{m_f}{2m}\right)\right]\right\}.
\end{aligned}$$

5.4 Final amplitude for p + p → p + p + f

Adding all contributions due to the exchange by scalar (f and a_0), pseudoscalar (π and η) and vector (ρ and ω) mesons, one obtains the following expression for the amplitude g_1, which describes the full threshold spin structure for the production of f_0-mesons in pp collisions:

$$\begin{aligned} g_1 = \frac{g^2_{NN\pi} g_{fNN}}{2m(t-m_\pi^2)} \Bigg\{ & -\left(\frac{|\mathbf{k}|}{E+m}\right)^2 \left(1 + 2\frac{g_{f\pi\pi}}{g_{fNN}}\right) \\ & + \left(\frac{|\mathbf{k}|}{E+m}\right)^2 \left(\frac{g_{\eta NN}}{g_{\pi NN}}\right)^2 \mathcal{R}_{\eta\pi}(t) \\ & - \left(\frac{g_{fNN}}{g_{\pi NN}}\right)^2 \mathcal{R}_{f\pi}(t) + \left(\frac{g_{a_0 NN}}{g_{\pi NN}}\right)^2 \mathcal{R}_{a\pi}(t) \\ & + \left(\frac{g_{\omega NN}}{g_{\pi NN}}\right)^2 \left(\frac{4k}{4m+m_f}\right) \\ & \times \left[1 - \kappa_\omega^2 + \left(1 - \kappa_\omega^2 \frac{m_f^2}{16m^2}\right)\frac{2m}{m_f}\right] \mathcal{R}_{\omega\pi}(t) \\ & - \left(\frac{g_{\rho NN}}{g_{\pi NN}}\right)^2 \left(\frac{4k}{4m+m_f}\right) \\ & \times \left[1 - \kappa_\rho^2 + \left(1 - \kappa_\rho^2 \frac{m_f^2}{16m^2}\right)\frac{2m}{m_f}\right] \mathcal{R}_{\rho\pi}(t) \Bigg\} , \end{aligned} \tag{37}$$

where $\mathcal{R}_{M\pi}(t) = (t-m_\pi^2)/(t-m_M^2)$, $M = \eta$, f, a_0, ρ or ω. Note that, in the considered model, the relative signs of all these contributions are fixed. We neglected, for simplicity, the t-channel contributions for processes others than $\pi + N \to N + f$. No information exists about the triple scalar interaction, g_{fff} and $g_{fa_0a_0}$, as well as on the g_{fVV} coupling constants. Therefore, these "exotic" contributions will be neglected in our numerical calculations, in order to reduce the possible ambiguities.

Taking the following numerical values for the coupling constants which enter in the expression (37):

$$\begin{gathered} g_{\pi NN} = 13.6, \quad g_{fNN} = 8.5 \text{ [23]}, \quad g_{a_0 NN} = 3.7 \text{ [50]}, \\ g_{\eta NN} \simeq 6 \text{ [51]}, \quad g_{\rho NN} = 3.04, \quad \kappa_\rho = 6.1 \text{ [47]}, \\ g_{\omega NN} = 13.7, \quad -0.3 < \kappa_\omega < +0.3 \text{ [52]} \end{gathered} \tag{38}$$

one finds the following parametrization for the threshold amplitude g_1:

$$g_1 = \frac{0.1}{m} \frac{g^2_{\pi NN} g_{fNN}}{(t-m_\pi^2)} \Sigma, \tag{39}$$

where

$$\begin{aligned} \Sigma = & -1 - 0.2\frac{g_{\pi\pi f}}{g_{fNN}} - 0.93^{(f)} + 0.33^{(a+\eta)} \\ & + (5.66\text{–}5.47)^{(\omega)} + 5.32^{(\rho)} \end{aligned}$$

and the upper indices refer to the individual t contribution. This evaluation allows to do the following considerations on the relative role of the different contributions to the amplitude g_1:

- The largest contributions, ρ and ω, have the same sign (note that a larger (smaller) value of the ω contribution corresponds to $\kappa_\omega = 0$ ($\kappa_\omega = \pm 0.3$).
- The η and a_0 contributions are one order of magnitude smaller than the individual ρ and ω contributions.
- The numerical value of g_1 depends strongly on the value of the coupling constant $g_{\omega NN}$, which can take values in the interval: $g^2_{\omega NN}/4\pi \simeq 8$–$35$ [51].

From $\Gamma(f \to 2\pi) = 40$–100 MeV, we find $|g_{f\pi\pi}| = 1.2$–1.9. Finally the sum of the different contributions can be written as

$$\Sigma_\pm = -1 \mp (0.28\text{–}0.45)^{(\pi)} - 0.6^{(f+a+\eta)} + (11\text{–}10.8)^{(\omega+\rho)},$$

so

$$\Sigma_\pm = \begin{cases} -(7.75\text{–}9.12), & \text{if } g_{f\pi\pi}/g_{fNN} > 0, \\ -(8.48\text{–}9.85), & \text{if } g_{f\pi\pi}/g_{fNN} < 0, \end{cases} \tag{40}$$

with small sensitivity on the value of κ_ω and on the sign of the ratio $g_{f\pi\pi}/g_{fNN}$. Finally,

$$|\Sigma|^2 = 60(1\text{–}1.6), \tag{41}$$

i.e. the cross-section of the process $p + p \to p + p + f_0$ can be predicted with good accuracy, in the framework of the considered model.

5.5 Effects of the form factors

Another important source of uncertainty in the calculation of the cross-section for scalar-meson production in NN collisions, is related to the choice of the phenomenological form factors in the hadronic vertices for the subprocesses $M^* + N \to N + f_0$. The symmetry of the s, u and t contributions does not hold, and the s, u terms do not partially cancel any longer. To prove this, let us consider the manifestation of the form factors for virtual nucleons:

$$F_N(s) = \frac{\Lambda_N^4}{\Lambda_N^4 + (s-m^2)^2} \text{ and } F_N(u) = \frac{\Lambda_N^4}{\Lambda_N^4 + (u-m^2)^2}, \tag{42}$$

where $\Lambda_N = (1.2\text{–}1.3)$ GeV is a cut-off parameter.

At threshold of any process $M + N \to N + f$, with s and u determined by eq. (26), we have

$$R_{su} = F_N(u)/F_N(s) = 1.82 \neq 1, \text{ for } \Lambda_N = 1.2 \text{ GeV} .$$

As a result this ratio affects essentially the relative role of s and u contributions:
For π and η:

$$\begin{aligned} (W+m)\left(\frac{1}{s-m^2} + \frac{1}{u-m^2}\right) = -\frac{1}{2m} \to \\ \frac{1}{m_f} - R_{su}\frac{W+m}{2mm_f} = -\frac{1.76}{m_f}, \end{aligned} \tag{43}$$

which gives an increase of a factor of three in absolute value.

For f and a_0:

$$\frac{2m+m_f}{s-m^2}+\frac{2m-m_f}{u-m^2}=\frac{1}{2m}\rightarrow$$
$$\frac{2m+m_f}{s-m^2}+R_{su}\frac{2m-m_f}{u-m^2}=\frac{0.13}{m_f}, \qquad (44)$$

i.e. in this case the resulting value, obtained including the form factors, is three times smaller.
For vector mesons:

$$h_{1V}\rightarrow-\frac{1.77}{m_f}(1+0.17\kappa_V),$$
$$h_{2V}\rightarrow-\frac{1.76}{m_f}(1+0.19\kappa_V). \qquad (45)$$

To estimate the effects of form factors for the amplitude g_1, let us assume, for simplicity, that all M^*NN-vertices can be characterized by a unique form factor $F(t)$. Then the amplitude g_1 can be written as follows:

$$g_1^{(F)}=g_{fNN}\frac{g^2_{\pi NN}}{t-m_\pi^2}\frac{0.37}{m_f}F^2(t)F_N(s)\Sigma_\pm^{(F)},$$
$$\Sigma_\pm^{(F)}=-1-2\frac{g_{\pi\pi f}}{g_{fNN}}\frac{F(t)}{F_N(s)}-0.09^{(f)}+0.015^{(a)}$$
$$+0.15^{(\eta)}+(6.2\text{–}5)^{(\omega)}-1.61^{(\rho)}, \qquad (46)$$

where the ω contribution is very sensitive to κ_ω (not only to the absolute value, but to the sign also):

$$\Sigma_\pm^{(F)}=\begin{cases}3.74-2\dfrac{g_{\pi\pi f}}{g_{fNN}}\dfrac{F(t)}{F_N(s)}, & \text{if } \kappa_\omega=+0.3,\\ 2.54-2\dfrac{g_{\pi\pi f}}{g_{fNN}}\dfrac{F(t)}{F_N(s)}, & \text{if } \kappa_\omega=-0.3\end{cases}$$

Taking, as an example, $F(t)=\Lambda^2/(\Lambda^2-t)$, with $\Lambda\simeq 1$ GeV, we find that the result will be more sensitive to the relative signs of the coupling constants $g_{\pi\pi f}$ and g_{fNN} than in the case where form factors were not taken into account:

$$\Sigma_+^{(F)}=(3.0\text{–}3.4),\ \ \Sigma_-^{(F)}=(4.4\text{–}4.8),\ \ \text{if } \kappa_\omega=+0.3,$$
$$\Sigma_+^{(F)}=(1.8\text{–}2.2),\ \ \Sigma_-^{(F)}=(3.2\text{–}3.6),\ \ \text{if } \kappa_\omega=-0.3, \qquad (47)$$

i.e. near threshold, the largest value of the cross-section for $p+p\rightarrow p+p+f_0$ is given by $\kappa_\omega=0.3$.

6 Threshold behavior of the cross-section

After calculating the different contributions to the matrix element for the process $p+p\rightarrow p+p+f_0$, we can estimate the cross-section in the near-threshold region. We start from the following expression [8]:

$$\sigma=\frac{1}{2}\mathcal{N}_f|\mathcal{M}|^2Q^2,$$
$$\mathcal{N}_f=\frac{m}{(2m+m_f)^2}\sqrt{\frac{m}{(2m+m_f)}}\frac{1}{|\mathbf{k}|}\frac{1}{256\pi^2}$$
$$\simeq 2.5\cdot 10^{-5}\ \ \text{GeV}^{-2}, \qquad (48)$$

where the coefficient $1/2$ takes into account the identity of the final protons in the considered process. The matrix element $\mathcal{M}$ can be written in the following form:

$$\mathcal{M}=1.39g_{fNN}\frac{g^2_{\pi NN}}{t-m_\pi^2}(E+m)F_N(s)F^2(t)\Sigma_\pm$$
$$\simeq 300\ \Sigma_\pm\ \ \text{GeV}^{-1}. \qquad (49)$$

The Q behavior of the cross-section can be finally written as

$$\sigma_{\text{th}}=0.45(Q/\text{GeV})^2\Sigma_\pm^2\ \text{mb}. \qquad (50)$$

This prediction can be compared to the existing experimental estimation [8]:

$$\sigma_{\text{exp}}(pp\rightarrow ppf_0\rightarrow ppK^+K^-)\simeq 2\ \text{nb at } Q=17\ \text{MeV}. \qquad (51)$$

Taking $\text{Br}(f_0\rightarrow K^+K^-)=1\%$, one can find $\sigma_{\text{exp}}=0.7\ \text{mb}(Q/\text{GeV})^2$. Comparing σ_{exp} and σ_{th}, one can conclude that $|\Sigma|\simeq 1$, which is more compatible with $\kappa_\omega=-0.3$ and a positive sign of the coupling constants $g_{\pi\pi f}$ and g_{fNN}.

The effects of the initial- and final-state interaction have been neglected in the previous estimations. If one assumes that the initial pp interaction induces a decreasing factor comparable with $p+p\rightarrow p+p+\eta'$, then larger values of Σ (which can be obtained for a negative value of κ_ω) seem preferable. However, the initial pp states for η' and f_0 production are different.

Finally, taking the following simple relation:

$$\frac{\sigma(pp\rightarrow ppa_0)}{\sigma(pp\rightarrow ppf_0)}\simeq\left(\frac{g_{a_0NN}}{g_{f_0NN}}\right)^2\simeq 1/6, \qquad (52)$$

it is possible also to predict the threshold behavior of a_0 production:

$$\sigma(pp\rightarrow ppa_0)\simeq 80(Q/\text{GeV})^2|\Sigma_\pm|^2\mu\text{b} \qquad (53)$$

and we find the same sensitivity to κ_ω. To be more rigorous, it would be necessary to use $g_{a_0\pi\eta}/g_{a_0NN}$ instead of $g_{f\pi\pi}/g_{fNN}$.

7 Comments on the NN final-state interaction (FSI)

In order to illustrate possible effects of FSI for the considered reaction, let us make an oversimplified estimation, using only the NN scattering length approximation, which will result in an upper limit for the NN FSI. Let us consider, for illustration, the case of pion exchange. One finds the following correction for some of the observables which have been previously discussed:

– The ratio of np and pp cross-sections:

$$R^{(\pi)}=\frac{1}{2}\left[\frac{a_s(np)}{a_s(pp)}\right]^2+\frac{27}{2}\left[\frac{a_t(np)}{a_s(pp)}\right]^2.$$

– The polarization effects for np collisions:

$$C_{nn}^{(\pi)} = \frac{9 - R_{st}^2}{27 + R_{st}^2},\ D_{nn}^{(\pi)} = \frac{6(R_{st} - 3)}{27 + R_{st}^2},$$

where $R_{st} = [a_s(np)/a_t(np)]$, $a_s(NN)$ is the singlet NN scattering length and $a_t(np)$ is the triplet np scattering length (for the S-state).

Using the following values for the scattering lengths [53]: $a_s(np) = -23.768$ fm, $a_t(np) = 5.424$ fm, and $a_s(pp) = -7.8098$ fm, one can find: $R^{(\pi)} \simeq 11$ (instead of 14), $C_{nn}^{(\pi)} \simeq= -0.22$ (instead of 0.29), and $D_{nn}^{(\pi)} \simeq -0.96$ (instead of -0.43), *i.e.* the final-state np interaction can change the sign of $C_{nn}^{(\pi)}$, but does not affect much the ratio $R^{(\pi)}$.

Note that the polarization observables are modified by FSI only near threshold, and therefore appear when the effective mass of the produced pp-system is known very precisely.

8 Conclusions

Let us summarize the main results concerning the production of scalar mesons in nucleon-nucleon collisions near threshold.

– We parametrized the spin structure of the threshold matrix element for the processes $p + p \to p + p + S^0$, where S^0 is a neutral scalar meson, $S = \sigma$, f_0, or a_0, in terms of a single spin structure, corresponding to a singlet-singlet transition in the pp-system. The same structure describes the production of the charged $a_0^{\pm}$-mesons in the processes $p + p \to p + n + a_0^+$ and $n + p \to p + p + a_0^-$.
– The process $n + p \to n + p + S^0$ is characterized by a more complicated spin structure, where the matrix element contains, in the general case, three contributions with different spin structures. One contribution coincides with the $\mathcal{M}(pp \to ppS^0)$ matrix element due to isotopic invariance, and two additional contributions describe the triplet-triplet transition in the np-system, which are forbidden by the Pauli principle, in case of the pp-system.
– The suggested model-independent parametrization of the spin structure, which is based on the general symmetry properties of the strong interaction (such as P-invariance, isotopic invariance, conservation of angular momentum and Pauli principle) allows to analyze polarization effects for pp and np collisions in a transparent way. These effects are very peculiar at threshold, where all final particles are emitted in relative S-state.
– The standard t-channel dynamics for the process $N + N \to N + N + S^0$ is generated by different meson exchanges with $\mathcal{J}^P = 0^+$ and $\mathcal{J}^P = 0^-$ and isotopic spin $\mathcal{I} = 0$ and $\mathcal{I} = 1$. The dependence of the polarization phenomena in $n + p \to n + p + S^0$ on the quantum number of the exchanged mesons can be described in terms of the corresponding S-channel partial amplitudes, with the help of the Fierz transformation in its two-component form.
– The resulting amplitude for $p+p \to p+p+f_0$ depends essentially on the coupling constants and on the form factors $F_N(s)$ and $F_N(u)$, which describe the effects of the nucleon virtuality.
– The processes $p+p \to p+p+S^0$ and $n+p \to n+p+S^0$ manifest large isotopic effects: the S-state production of scalar mesons is larger in np collisions than in pp collisions and polarization phenomena are different.

Note that these results do not depend on the structure of the f_0- and a_0-mesons ($q\overline{q}$ states, four-quark state, $K\overline{K}$-molecule etc.) and on the mechanisms of their decays.

References

1. F.E. Close, Y.L. Dokshitzer, V.N. Gribov, V.A. Khoze, M.G. Ryskin, Phys. Lett. B **319**, 291 (1993).
2. M. Genovese, Nuovo Cimento A **107**, 1249 (1994).
3. G. Janssen, B.C. Pearce, K. Holinde, J. Speth, Phys. Rev. D **52**, 2690 (1995).
4. V.V. Anisovich, A.V. Sarantsev, A.A. Kondashov, Y.D. Prokoshkin, S.A. Sadovsky, Phys. Lett. B **355**, 363 (1995).
5. K. Maltman, Nucl. Phys. A **675**, 209c (2000).
6. S. Narison, Nucl. Phys. A **675**, 54c (2000); Nucl. Phys. Proc. Suppl. **86**, 242 (2000).
7. F.E. Close, A. Kirk, Phys. Lett. B **489**, 24 (2000).
8. P. Moskal, M. Wolke, A. Khoukaz, W. Oelert, Prog. Part. Nucl. Phys. **49**, 1 (2002).
9. B. Friman, M. Soyeur, Nucl. Phys. A **600**, 477 (1996).
10. Q. Zhao, Z. Li, C. Bennhold, Phys. Rev. C **58**, 2393 (1998); Phys. Lett. B **436**, 42 (1998).
11. A.I. Titov, T.S.H. Lee, H. Toki, O. Streltsova, Phys. Rev. C **60**, 035205 (1999).
12. M. Chemtob, E.J. Moniz, M. Rho, Phys. Rev. C **10**, 344 (1974).
13. E. Hummel, J.A. Tjon, Phys. Rev. Lett. **63**, 1788 (1989); Phys. Rev. C **42**, 423 (1990).
14. J.W. Van Orden, N. Devine, F. Gross, Phys. Rev. Lett. **75**, 4369 (1995).
15. G.A. Miller, S.J. Brodsky, M. Karliner, Phys. Lett. B **481**, 245 (2000).
16. HERMES Collaboration (K. Ackerstaff *et al.*), Phys. Lett. B **475**, 386 (2000).
17. M.N. Achasov *et al.*, JETP Lett. **71**, 355 (2000) (Pis'ma Zh. Eksp. Teor. Fiz. **71**, 519 (2000)).
18. A.V. Anisovich, V.V. Anisovich, D.V. Bugg, V.A. Nikonov, Phys. Lett. B **456**, 80 (1999).
19. M. Boglione, M.R. Pennington, Eur. Phys. J. C **9**, 11 (1999).
20. Z.P. Li, F.E. Close, T. Barnes, Phys. Rev. D **43**, 2161 (1991).
21. M. Vanderhaeghen, Phys. Lett. B **368**, 13 (1996).
22. C. Elster, K. Holinde, R. Machleidt, Phys. Rep. **149**, 1 (1987).
23. V. Mall, K. Holinde, R. Machleidt, Phys. Rev. C **51**, 2360 (1995).
24. E.L. Bratkovskaya, W. Cassing, L.A. Kondratyuk, A. Sibirtsev, Eur. Phys. J. A **4**, 165 (1999).
25. V.Y. Grishina, L.A. Kondratyuk, E.L. Bratkovskaya, M. Büscher, W. Cassing, Eur. Phys. J. A **9**, 277 (2000); V.Y. Grishina, L.A. Kondratyuk, M. Büscher, W. Cassing, H. Stroher, Phys. Lett. B **521**, 217 (2001).

26. H. Muller, Eur. Phys. J. A **11**, 113 (2001).
27. A.E. Kudryavtsev, V.E. Tarasov, JETP Lett. **72**, 410 (2000) (Pis'ma Zh. Eksp. Teor. Fiz. **72**, 589 (2000)).
28. A.E. Kudryavtsev, V.E. Tarasov, J. Haidenbauer, C. Hanhart, J. Speth, Phys. Rev. C **66**, 015207 (2002).
29. O.I. Dahl, L.M. Hardy, R.I. Hess, J. Kirz, D.H. Miller, J.A. Schwartz, Phys. Rev. **163**, 1430 (1967); **183**, 1520 (1969) (E).
30. W. Beusch *et al.*, Phys. Lett. B **25**, 357 (1967).
31. A.J. Pawlicki, D.S. Ayres, R. Diebold, A.F. Greene, S.L. Kramer, A.B. Wicklund, Phys. Rev. D **12**, 631 (1975).
32. N.M. Cason *et al.*, Phys. Rev. Lett. **41**, 271 (1978).
33. D. Cohen, D.S. Ayres, R. Diebold, S.L. Kramer, A.J. Pawlicki, A.B. Wicklund, Phys. Rev. D **22**, 2595 (1980).
34. A. Etkin *et al.*, Phys. Rev. D **25**, 2446 (1982).
35. DISTO Collaboration (F. Balestra *et al.*), Phys. Rev. C **63**, 024004 (2001); Phys. Rev. Lett. **81**, 4572 (1997); Phys. Lett. B **468**, 7 (1999).
36. C. Quentmeier *et al.*, Phys. Lett. B **515**, 276 (2001).
37. W. Oelert, Proposal for the COSY-11 facility, COSY (1988).
38. M. Büscher *et al.*, COSY proposal No. 97 (2001), `http://www.fz-juelich.de/ikp/anke`.
39. P. Moskal, W. Oelert, in *Proceedings of the Symposium on Threshold Meson Production in pp and pd Interaction (COSY-11), Cracow, Poland, 20-24 June 2001*, edited by P. Moskal, M. Wolke, *Schriften des Forschungszentrums Jülich, Matter and Materials*, Vol. **11** (FZ Jülich, Jülich, 2002) p. 212; P. Moskal, ibidem, p. 27, arXiv:nucl-ex/0110001 .
40. E. Tomasi-Gustafsson, M.P. Rekalo, Phys. Part. Nucl. **33**, 220 (2002) (Fiz. Elem. Chastits At. Yadra **33**, 436 (2002)).
41. M.P. Rekalo, J. Arvieux, E. Tomasi-Gustafsson, Z. Phys. A **357**, 133 (1997).
42. M.P. Rekalo, J. Arvieux, E. Tomasi-Gustafsson, Phys. Rev. C **55**, 2630 (1997).
43. M.P. Rekalo, J. Arvieux, E. Tomasi-Gustafsson, Phys. Rev. C **56**, 2238 (1997).
44. M.P. Rekalo, E. Tomasi-Gustafsson, New J. Phys. **4**, 68 (2002).
45. M.P. Rekalo, E. Tomasi-Gustafsson, Eur. Phys. J. C **16**, 575 (2003).
46. V. Bernard, N. Kaiser, Ulf-G. Meissner, Eur. Phys. J. A **4**, 259 (1999).
47. R. Machleidt, Adv. Nucl. Phys. **19**, 189 (1989).
48. M. Benmerrouche, N.C. Mukhopadhyay, J.F. Zhang, Phys. Rev. D **51**, 3237 (1995).
49. W.T. Chiang, S.N. Yang, L. Tiator, D. Drechsel, Nucl. Phys. A **700**, 429 (2002).
50. M. Kirchbach, D.O. Riska, Nucl. Phys. A **594**, 419 (1995).
51. K. Nakayama, J. Speth, T.S. Lee, Phys. Rev. C **65**, 045210 (2002).
52. K. Nakayama, A. Szczurek, C. Hanhart, J. Haidenbauer, J. Speth, Phys. Rev. C **57**, 1580 (1998).
53. O. Dumbrajs, R. Koch, H. Pilkuhn, G.C. Oades, H. Behrens, J.J. De Swart, P. Kroll, Nucl. Phys. B **216**, 277 (1983).